Evidence of vacancy-induced surface states for nonstoichiometric $TiN_x(100)$

J. Redinger* and P. Weinberger
Institut für Technische Elektrochemie, Technische Universität Wien, A-1060 Wien, Austria
(Received 13 June 1986)

Angle-resolved photoemission spectra for nonstoichiometric $TiN_x(100)$ are calculated with use of a model for a vacancy-concentration gradient near or at the surface. From our model calculations a vacancy-induced surface state is found, which is similar to a Tamm surface state occurring frequently for stoichiometric surfaces.

INTRODUCTION

It is well known that rocksalt-type transition-metal carbides and nitrides hardly exist in a stoichiometric composition. Phases like TiN_x exist in many cases in which the transition-metal sublattice is completely occupied and the vacancies are distributed randomly over the nonmetal sublattice only. Although the presence of vacancies profoundly changes the physical properties of this technologically rather important class of compounds, comparatively little work has been devoted to gain some insight into vacancy-induced effects in the electronic structure of transition-metal carbides and nitrides.

Very recently, calculated x-ray-photoemission spectroscopy (XPS) spectra for nonstoichiometric refractory phases,[1] which are based on Korringa-Kohn-Rostoker coherent-potential-approximation (KKR-CPA) results,[2,3] showed impressively enough the vacancy-induced features found in the experimental data.[4–7] Especially for vacancy concentrations less than 20 at.% the agreement with the experimental spectra is excellent. In particular, in the case of TiN new experimental and theoretical Ti K x-ray emission spectroscopy (XES) spectra,[8] which map the Ti p—like density of states (DOS) only, gave a direct proof of the vacancy-induced states. It is important to note at this stage, that both experimental techniques—XPS and particularly XES—yield information about the electronic structure of the bulk.

The situation is quite different, however, in the case of angle-integrated or angle-resolved uv-photoelectron spectroscopy (ARUPS) spectra. Due to the rather low probing depth of uv-excited photoelectrons, the surface region contributes significantly to the intensity of the photocurrent. ARUPS have been obtained from nonstoichimetric $TiN_x(100)$,[9] $TiC_x(100)$,[10,11] $TiC_x(110)$,[10] $TiC_x(111)$,[10–12] $ZrN_x(100)$,[13] $VN_x(100)$,[14] and $NbN_x(100)$ (Ref. 14) single-crystal surfaces. In none of these spectra is any direct evidence for vacancy-related structures. Instead, a Tamm surface state has been experimentally detected in the cases of $TiN_x(100)$ (Ref. 15) and $ZrN_x(100)$.[16] Theoretical calculations showing Tamm surface states have been reported for the stoichiometric systems TiN(100) (Refs. 17–19) and TiC(100).[20]

In contrast to the single-crystal ARUPS, a completely different picture emerges from angle-integrated UPS spectra obtained from polycrystalline TiN_x and ZrN_x samples.[21] There are no surface-induced states, but a vacancy-induced feature is clearly visible at photon energies of about 40 eV. These findings have to be compared with the angle-integrated He II (40.8 eV) spectra[22] of the TiN(100) single-crystal used in the ARUPS experiments showing no vacancy states for the $TiN_{0.83}(100)$ single-crystal surface at all. The situation is even more controversial in view of our recent theoretical ARUPS (Ref. 23) from substoichiometric $TiN_x(100)$ surfaces, which clearly showed that a vacancy-induced peak should appear in normal emission at about -2 eV and photon energies above 36 eV. Most recent measurements[24] on $ZrN_x(100)$ do in fact show such vacancy-related structures, in good agreement with theory.[25]

In the case of typical uv wavelengths, such as Ne I or He I, the -2-eV peak is observable in off-normal emission for takeoff angles larger than 10°.

The question appears to be as follows: What happens to the vacancy-induced peaks if the vacancies are dying out towards the surface?

In order to give a more definite answer to this rather delicate question, we used a model for a vacancy-concentration gradient at or near the surface for the calculation of the present ARUPS. All theoretical ARUPS shown in the present communication (cf. Ref. 23) are based on Pendry's inverse-LEED (low-energy electron-diffraction) formalism,[26–30] treating disorder along the lines of Durham[31] and Schadler *et al.*[32] Bulk lattice parameters and bulk KKR-CPA scattering amplitudes[2] are used for all spectra shown. Since no *ab initio* surface KKR-CPA calculations are available, we used bulk KKR-CPA effective scattering amplitudes for the various disordered layers. It should be noted that the potentials used for the calculation of the various effective KKR-CPA scattering amplitudes[2] are those of stoichiometric TiN. Such a procedure seems to be well suited for the present purpose, since from a self-consistent augmented-plane-wave (APW) supercell calculation for $TiC_{0.75}$ (Ref. 33) and $TiN_{0.75}$,[34] the deviations from the stoichiometric potentials are found to be rather small. So, only different concentrations of vacancies in different layers will lead to layer-dependent scattering properties. In the case of stoichiometric top layers, we also investigated the influence of a shifted nitrogen potential for the surface. Guided by the results in Ref. 23, we have chosen a normal-emission geometry and, unless otherwise indicated, unpo-

larized He II (40.8 eV) radiation. The angle of incidence θ_i of the photons relative to the surface normal is 45°, thus allowing emission from both Δ_1-like and Δ_5-like initial states.

RESULTS

In Fig. 1 we show as a reference the spectra for "pure" $TiN_x(100)$. Here, and in all further cases, "pure" means that no vacancy-concentration gradient is present. The zero of energy (Fermi level) depends on x.[9] The Fermi level for $x=1.0$ is 0.25 eV higher than that for $x=0.83$. For $x=0.92$ the Fermi level is 0.1 eV higher than in $x=0.83$. Figures 1(a) and 1(b) show the HeII normal-emission spectra for $TiN_{0.83}(100)$ and $TiN_{0.92}(100)$, respectively. We find four prominent peaks, lying at about -5, -3, -2 eV, and close to the Fermi level. They have been identified in Ref. 23 as being due to emission from Δ_1-like and Δ_5-like N p initial states, Δ_1-like vacancy states, and Ti-d-band Δ_5-like initial states, respectively. The vacancy peak at -2 eV is missing in Fig. 1(c) for stoichiometric TiN(100) and a surface state appears in Fig. 1(d) instead, if the nitrogen top-layer potential is modified.[18,19] Although the Fermi level is higher for TiN(100) and $TiN_{0.92}(100)$, the energetic position of the -3-eV Δ_5-like emission is almost the same as for $TiN_{0.83}(100)$. In the case of $TiN_{0.92}(100)$, the peak is shifted by 0.1 eV even closer to the Fermi level. Consequently, on an absolute energy scale with respect to a layer-independent common muffin-tin zero, this peak moves closer to the Fermi edge with decreasing vacancy concentration. This shift is also reflected in the effective phase shifts at the nitrogen sublattice. In the vicinity of the -3-eV peak, the imaginary part of the phase shift is small, so it seems to be sufficient to concentrate on the real part only. Applying the usual resonance criterion for single-site scattering, one finds a shift of the resonance energy toward the Fermi level with decreasing vacancy concentration. This behavior is also related to the narrowing of the N-p-band DOS with increasing vacancy content. These findings are important in view of the spectra shown in Fig. 2, where Fig. 2(a)—"pure" $TiN_{0.83}(100)$—serves as a reference, and all the other spectra are given with respect to the Fermi level of $TiN_{0.83}$. Spectrum 2(b) reflects the situation of one layer of $TiN_{0.92}(100)$ on top of $TiN_{0.83}(100)$. Spectrum 2(c) is obtained if a second—stoichiometric—overlayer is included. Figure 2(d) is analogous to Fig. 2(c); only the stoichiometric nitrogen top-layer potential is now shifted by 0.4 eV.

In the following we will concentrate our arguments on the energy region between -3 and -2 eV. The spectrum for "pure" $TiN_{0.83}(100)$—2(a)—shows two peaks, which are seen in Fig. 2(b) only as shoulders of a new peak at -2.5 eV. This particular peak is a Tamm-like surface state due to the different scattering properties in the top

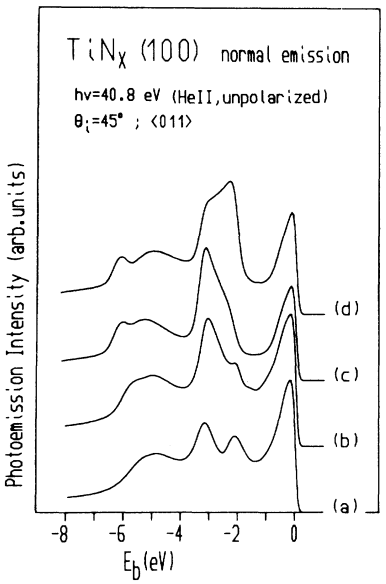

FIG. 1. Calculated normal-emission spectra for stoichiometric and substoichiometric $TiN_x(100)$. Unpolarized He II radiation (40.8 eV) is incident along the ΓULK azimuth at an angle $\theta_i=45°$ with respect to the surface normal: (a) $x=0.83$, (b) $x=0.92$, (c) $x=1.00$, and (d) $x=1.00$(s). (s) denotes nitrogen top-layer potential shifted by 0.4 eV; cf. Refs. 18 and 19.

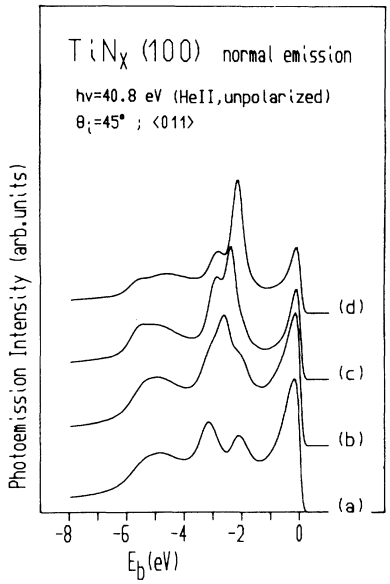

FIG. 2. Calculated normal-emission spectra for substoichiometric $TiN_x(100)$ displaying a vacancy-concentration gradient in the surface region. Unpolarized He II radiation (40.8 eV) is incident along the ΓULK azimuth at an angle $\theta_i=45°$ with respect to the surface normal:

	Top layer	Top -1 layer	Bulk
(a)	$x=0.83$	$x=0.83$	$x=0.83$
(b)	$x=0.92$	$x=0.83$	$x=0.83$
(c)	$x=1.00$	$x=0.92$	$x=0.83$
(d)	$x=1.00$(s)	$x=0.92$	$x=0.83$

(s) denotes nitrogen top-layer potential shifted by 0.4 eV; cf. Refs. 18 and 19.

layer caused by a different vacancy concentration in the top layer. It therefore makes sense to speak of a vacancy-induced surface state. In Fig. 2(c), again there is only a two-peak structure. The original bulklike vacancy-induced peak at -2 eV is strongly overshadowed by the vacancy-induced surface state and is barely visible as a slight shoulder. The shoulder disappears completely if a shifted top-layer potential is used [Fig. 2(d)]. It is clear that a shifted nitrogen top-layer potential will increase the splitting off of the vacancy-induced surface state. This can be seen from the increased intensity of the surface-state peak by comparing the spectra of Figs. 2(c) and 2(d). Furthermore, the energetic position of both peaks is shifted closer to the Fermi edge, since in this case, due to the small escape depth of the photoelectrons, the bulklike bands are also seen to be affected.

Figure 3 illustrates the behavior of a vacancy-induced surface state. In Fig. 3 "pure" $TiN_{0.92}(100)$—3(a)—serves as a scale of reference. The other cases shown are (i) one stoichiometric layer on top of $TiN_{0.92}(100)$ [Fig. 3(b)], (ii) two stoichiometric layers on top of $TiN_{0.92}(100)$ [Fig. 3(c)], and (iii) two stoichiometric overlayers on top of $TiN_{0.92}(100)$ with the top-layer nitrogen potential shifted [Fig. 3(d)]. The bulklike vacancy state is hidden behind the vacancy-induced surface state already for one stoichiometric top layer [Fig. 3(b)]. It seems, therefore, to be an unavoidable necessity to have vacancies in the top layer, in order to see vacancy-related features in the AR-UPS from a single-crystalline $TiN_x(100)$ samples. If a second stoichiometric layer is put on top, the intensity of the induced surface state is decreased with respect to the bulk states [Fig. 3(c)]. This peak, however, is enhanced again if a shifted top-layer potential is taken into account [Fig. 3(d)]. This has the same effect as a concentration gradient, as stated already above.

In order to gain some insight into the polarization dependence of the vacancy-induced surface state, in Fig. 4 all spectra shown correspond to $TiN_{0.92}(100)$ with a single stoichiometric top layer. Using a shifted top-layer potential [Fig. 4(b)], the surface state gains intensity and is shifted closer to the Fermi level. Changing the angle of incidence θ_i of the impinging He II photons from 45° to 15° and using an unshifted top-layer potential [Fig. 4(c)], we find close agreement with Fig. 4(a). As compared to Fig. 4(a), the smaller θ_i in Fig. 4(c) reduces the transition probability from Δ_1-like initial states. As can be seen quite clearly, only the peak around -5 eV is seriously affected. There is also a slight narrowing of the double

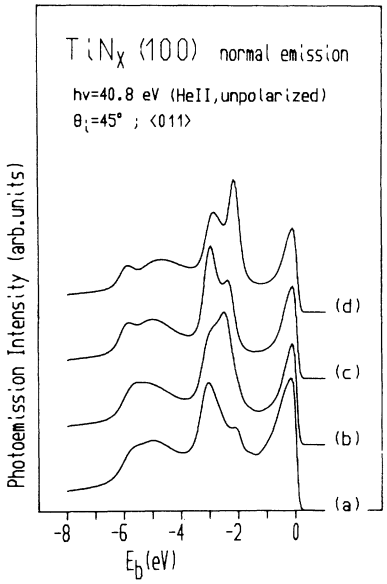

FIG. 3. Calculated normal-emission spectra for sub-stoichiometric $TiN_x(100)$ displaying a vacancy-concentration gradient in the surface region. Unpolarized He II radiation (40.8 eV) is incident along the ΓULK azimuth at an angle $\theta_i = 45°$ with respect to the surface normal:

	Top layer	Top -1 layer	Bulk
(a)	$x=0.92$	$x=0.92$	$x=0.92$
(b)	$x=1.00$	$x=0.92$	$x=0.92$
(c)	$x=1.00$	$x=1.00$	$x=0.92$
(d)	$x=1.00$(s)	$x=1.00$	$x=0.92$

(s) denotes nitrogen top-layer potential shifted by 0.4 eV; cf. Refs. 18 and 19.

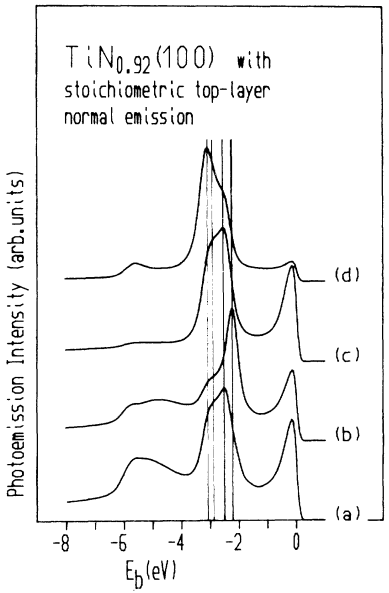

FIG. 4. Calculated normal-emission spectra for sub-stoichiometric $TiN_{0.92}(100)$ displaying a vacancy-concentration gradient—stoichiometric top layer—at the surface. In the case of spectrum (b), the nitrogen top-layer potential was shifted by 0.4 eV; cf. Refs. 18 and 19. Except for spectrum (d), unpolarized He II radiation (40.8 eV) is incident along the ΓULK azimuth. The angle of incidence θ_i with respect to the surface normal is 45° for spectra (a) and (b) and 15° for spectra (c) and (d). In the case of spectrum (d), p-polarized light with an energy of 17 eV is incident along the ΓXWK azimuth.

peak extending between -3 and -2 eV, due to the loss of intensity of the Δ_1-like vacancy-related shoulder in Fig. 4(c). The intensity ratio of the bulk N-p-Δ_5-like peak and the vacancy-induced surface-state emission is left unchanged, so that the initial states show the same symmetry, namely Δ_5. This behavior indeed supports the above-given arguments for a vacancy-induced surface state, split off from the N-p-bulk bands, similar to a Tamm surface state. Using a different source of radiation, namely 17 eV p-polarized photons, Fig. 4(d) is obtained. In Fig. 4(d) the surface state remains at the same energy as in Fig. 4(c), but the bulk states have shifted to larger binding energies. If Fig. 4 is compared to the spectrum obtained for stoichiometric TiN(100) with a shifted top-layer potential [see Fig. 1(b) of Ref. 18], one finds almost no differences between these two cases and, in turn, with the experimental spectrum [see Fig. 1(c) of Ref. 18]. This statement is rather important recalling the fact that no vacancy-related features, but a surface state, has been identified in the experimental ARUPS of nominal $TiN_{0.83}(100)$. In view of our present results, modeling a vacancy-concentration gradient at the surface, such experimental findings are no longer surprising, since already one stoichiometric top layer is sufficient to rub out the bulklike vacancy-state emission in favor of emission from a vacancy-induced surface state. However, the two states may be unambiguously identified from their polarization dependence, since the vacancy state shows Δ_1-like and the induced surface state Δ_5-like symmetry.

CONCLUSIONS

The limitations of the applied model for the vacancy gradient are quite clear: (i) Since there are at present no layer KKR-CPA calculations for semi-infinite crystals with different concentrations in different layers available, bulklike KKR-CPA scattering amplitudes are used. (ii) three different concentrations, namely $x=0.83$, 0.92, and 1.0, are only a rough measure for a concentration gradient. The present model calculations, however, do show that a vacancy gradient can indeed have an important effect on ARUPS: The model calculations show a vacancy-induced surface state split off from the N-p-Δ_5—like states, similar to the Tamm surface state for the stoichiometric surface. In contrast to the Δ_5-like vacancy-induced surface states, the vacancy-induced states themselves are bulklike in nature and show Δ_1-like symmetry. This different initial-state symmetry offers a chance to distinguish unambiguously between the two vacancy-related features by examining their polarization dependence. Provided that there are enough vacancies left at the surface,[35] vacancy states should be observable in ARUPS of substoichiometric $TiN_x(100)$ and in related systems.

ACKNOWLEDGMENTS

This work was supported by the Austrian Fonds zur Förderung der wissenschaftlichen Forschung, Projekt Nr. P5543.

*Present address: Department of Physics, Northwestern University, Evanston, IL 60201.

[1]J. Redinger, P. Marksteiner, and P. Weinberger, Z. Phys. B **63**, 221 (1986).
[2]P. Marksteiner, P. Weinberger, A. Neckel, R. Zeller, and P. H. Dederichs, Phys. Rev. B **33**, 812 (1986).
[3]P. Marksteiner, P. Weinberger, A. Neckel, R. Zeller, and P. H. Dederichs, Phys. Rev. B **33**, 6709 (1986).
[4]H. Höchst, P. Steiner, S. Hufner, and C. Politis, Z. Phys. B **37**, 27 (1980).
[5]H. Höchst, R. D. Bringans, P. Steiner, and Th. Wolf, Phys. Rev. B **25**, 7183 (1982).
[6]L. Porte, L. Roux, and J. Hanus, Phys. Rev. B **28**, 3214 (1983).
[7]L. Porte, Solid State Commun. **50**, 303 (1984).
[8]E. Beauprez, C. F. Hague, J.-M. Mariot, F. Teyssandier, J. Redinger, P. Marksteiner, and P. Weinberger, Phys. Rev. B **34**, 886 (1986).
[9]L. I. Johansson, A. Callenås, P. M. Stefan, A. N. Christensen, and K. Schwarz, Phys. Rev. B **24**, 1883 (1981).
[10]A. Callenås, L. I. Johansson, A. N. Christensen, K. Schwarz, and J. Redinger, Phys. Rev. B **27**, 5934 (1983).
[11]J. H. Weaver, A. M. Bradshaw, J. F. van der Veen, F. J. Himpsel, D. E. Eastman, and C. Politis, Phys. Rev. B **22**, 4921 (1980).
[12]A. M. Bradshaw, J. F. van der Veen, F. J. Himpsel, and D. E. Eastman, Solid State Commun. **37**, 37 (1980).
[13]A. Callenås, L. I. Johansson, A. N. Christensen, K. Schwarz, P. Blaha, and J. Redinger, Phys. Rev. B **30**, 635 (1984).
[14]A.Callenås, L. I. Johansson, A. N. Christensen, K. Schwarz, and P. Blaha, Phys. Rev. B **32**, 575 (1985).
[15]L. I. Johansson and A. Callenås, Solid State Commun. **42**, 299 (1981).
[16]A. Callenås and L. I. Johansson, Solid State Commun. **52**, 143 (1984).
[17]J. E. Inglesfield, A. Callenås, and L. I. Johansson, Solid State Commun. **44**, 1321 (1982).
[18]C. G. Larsson, L. I. Johansson, and A. Callenås, Solid State Commun. **49**, 727 (1984).
[19]L. I. Johansson, C. G. Larsson, and A. Callenås, J. Phys. F **14**, 1761 (1984).
[20]J. Redinger, P. Weinberger, E. Wimmer, A. Neckel, and A. J. Freeman, Phys. Rev. B **32**, 6993 (1985).
[21]R. D. Bringans and H. Höchst, Phys. Rev. B **30**, 5416 (1984).
[22]L. I. Johansson, P. M. Stefan, M. L. Shek, and A. N. Christensen, Phys. Rev. B **22**, 1032 (1980).
[23]J. Redinger, P. Weinberger, and A. Neckel, preceding paper, Phys. Rev. B **35**, 5647 (1987).
[24]J. Lindström, L. I. Johansson, A. Callenås, D. S. L. Law, and A. N. Christensen (unpublished).
[25]J. Redinger, Solid State Commun. **61**, 133 (1987).
[26]J. B. Pendry, *Low Energy Electron Diffraction* (Academic, New York, 1974).
[27]J. B. Pendry, Surf. Sci. **57**, 679 (1976).
[28]J. F. L. Hopkinson, J. B. Pendry, and D. J. Titterington, Comput. Phys. Commun. **19**, 69 (1980).
[29]P. J. Durham, W. M. Temmerman, C. G. Larsson, and P. O. Nilsson, Vacuum **33**, 771 (1983).
[30]C. G. Larsson, Surf. Sci. **152/153**, 213 (1985).

[31]P. J. Durham, J. Phys. F **11**, 2475 (1981).
[32]G. Schadler, P. Weinberger, A. Gonis, and J. Klima, J. Phys. F **15**, 1675 (1985).
[33]J. Redinger, R. Eibler, P. Herzig, A. Neckel, R. Podloucky, and E. Wimmer, J. Phys. Chem. Solids **46**, 383 (1985).
[34]P. Herzig, J. Redinger, R. Eibler, and A. Neckel, in Proceedings of the Eighth International Conference on Solid Compounds of Transition Elements, April 9—13, 1985, Vienna, Austria (Extended Abstracts P2B2) (unpublished).
[35]M. Aono, Y. Hou, R. Souda, C. Oshima, S. Otani, and Y. Ishizawa, Phys. Rev. Lett. **50**, 1293 (1983).